XPS ANALYSIS OF OXIDE TRANSFORMATION DURING SINTERING OF CHROMIUM ALLOYED PM STEELS

M. Vattur Sundaram, E. Hryha, L. Nyborg

Abstract

Water atomized PM steels prealloyed with chromium are becoming more and more widely used due to their high performance characteristics and sinter-hardening capabilities. Due to its low cost and recyclability, chromium is a cost effective alloying alternative to replace expensive and toxic Ni and non-recyclable Cu that are traditionally used in PM. Chromium has higher affinity towards oxygen that brings risk of formation of stable oxides that are difficult to reduce and hence inhibit the development and the growth of inter-particle necks during sintering. This in turn directly influences the strength of the compacts. In this study, the analysis of the change in oxide state after delubrication and during heating stage until sintering temperature was performed by means of surface sensitive analytical techniques such as XPS and high resolution SEM combined with EDX analysis. Composition, morphology and distribution of the oxides was estimated on the fracture surface of the compacts, based on powder prealloyed with 1.8 wt. % Cr, in the as-delubricated condition and sampled during the heating stage at 700, 900 and 1120 °C. Sintering atmosphere applied was dry 90% N_2/10% H_2 atmosphere (dew point ~-50 °C). The results show enrichment of surface oxides in Cr and Mn at around 900 °C during heating stage followed by their significant reduction close to the sintering temperature. This study provides the important details for tailoring the sintering process in terms of proper atmosphere and process control for chromium alloyed powder.

Keywords: prealloyed steel powder, surface oxides, oxides transformation, particulate oxides, XPS, SEM, sintering atmosphere control

INTRODUCTION

Chromium prealloyed powder is subjected to an annealing process in a reducing atmosphere after water atomization with the aim to reduce the surface oxides formed. From previous studies on chromium prealloyed powders [1,2] it has been found that the surface of the annealed powder is covered by heterogeneous oxide layer, which includes an Fe-oxide layer with a thickness in the range of 6-7 nm and oxide particulates rich in Cr-Mn-Si. The Fe-oxide layer covers the dominant part of the surface (about 95%). Hence, to facilitate effective growth of the inter particle necks during sintering, the surface iron oxide first has to be reduced, which is typically achieved by sintering in a reducing atmosphere containing hydrogen [3–5]. Reduction of the Fe-oxide by hydrogen takes place at around 350-550 °C, while the carbothermal reduction takes place at temperatures above 800 °C [5–11]. Sintering at higher temperatures often leads to the reduction of individual elements of the

Maheswaran Vattur Sundaram, Eduard Hryha, Lars Nyborg, Department of Materials and Manufacturing Technology, Chalmers University of Technology, Gothenburg, Sweden

spinel Cr-Mn-Si-rich oxide based on the stability at the respective temperature for conditions encountered.

MATERIALS AND METHODS

Water atomized Cr prealloyed powder of trade name Astaloy CrA (Fe-1.8 wt. % Cr) from Höganäs AB, Sweden, is used in this study. The powder was admixed with 0.5 wt. % graphite as a carbon source and 0.6 wt. % Kenoloube lubricant. The admixed powder was compacted into modified Charpy bars (5x10x55 mm^3) at 600 MPa to a green density of ~7.0 $g.cm^{-3}$ and sintered using 90% N_2/10% H_2 in a laboratory tube furnace with an estimated dew point of ~-50 °C. Prior to the sintering, de-lubrication was carried out at 450 °C for 30 minutes in dry N_2 atmosphere (dew point of ~-45 °C). Specimens were sampled at different stages of sintering as shown in Table 1.

Tab.1. Specimens sampled at different temperature throughout the sintering stages.

Temperature [°C]	450	700	900	1120	1120
Time [min]	30	1	1	1	30
Designation	CrA 450-30	CrA 700-1	CrA 900-1	CrA 1120-1	CrA 1120-30

The specimens were fractured by impact test and the fracture surfaces were analysed by X-ray photoelectron spectroscopy (XPS) using a PHI 5500 instrument. Fractographic studies were performed utilizing high resolution scanning electron microscopy (LEO Gemini 1550) combined with EDX analysis using an INCA-Energy analyser. The XPS investigation was combined with the compositional depth profiling by means of alternating Ar^+ etching and XPS analysis at the approximate depths of 1, 3, 5, 7.5, 10 and 20 nm. The depths quoted refer to the Ta_2O_5 units. This procedure provided an estimate of surface chemical composition and chemical state information vs. etch depth for the specimens studied.

RESULTS AND DISCUSSION

The spectra shown in Fig.1 are obtained after etching of 1 nm in order to avoid contribution from the adsorbed species. It is shown that Si, C, N, O, Mn, Cr and Fe are present on the surface with the traces of Si. The presence of Zn (Zn2p at ~1022 eV) after heating at 450 and 700 °C (see Fig.2a & 2b) is connected to the presence of residues of lubricant. However, it has to be taken into consideration that the XPS analysis is performed on samples fractured in air. Hence, there is re-oxidation and formation of the thin iron oxide layer (~3-4 nm) on the pure metallic surface. This fact is mainly responsible for the oxygen peak found on all sample surfaces analysed. To depict the presence of oxide inclusions inside sinter necks, this is indicated from measured surface content of strong oxide formers like Mn, Cr and Si.

To determine the thickness of the Fe-oxide layer, the Fe peak for all samples and etch depths was curve-fitted to quantify the contributions from metallic and oxide states, from which the Fe-metal intensity for each of the cases was calculated. The apparent oxide thickness, see Fig.3, was estimated based on the 65 % relative intensity value of the metal peak. This approach is based on the model describing effect of the ion etching on the relative intensity of the metal peak in case of metal powders, described elsewhere [12]. The values obtained are 7.5 nm, 5.4 nm and 5.3 nm for samples heated to 450 °C, 700 °C and 900 °C, respectively.

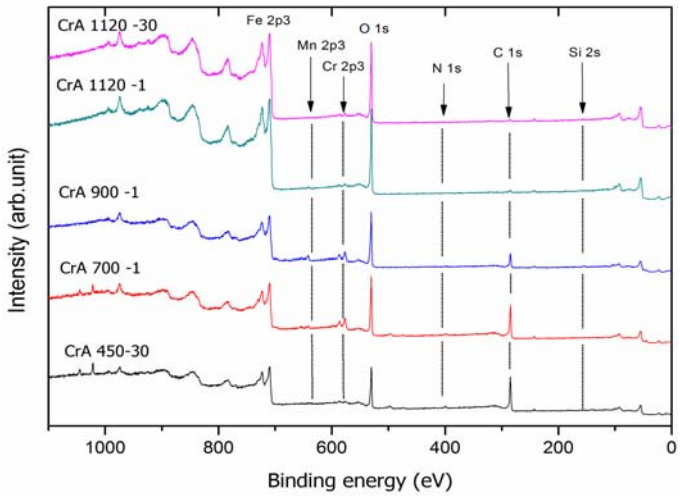

Fig.1. XPS survey spectra from the fractured surface after ion etching of 1 nm for the compacted samples subjected to different heating sequences as in Table 1.

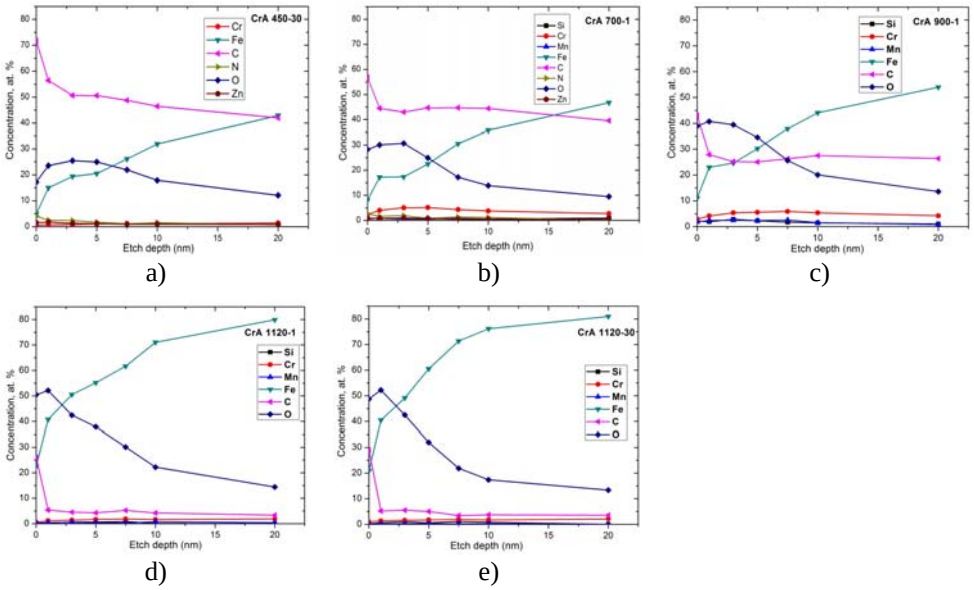

Fig.2. Chemical compositions of fractured samples heated to different temperatures as a function of etch depth (a-e).

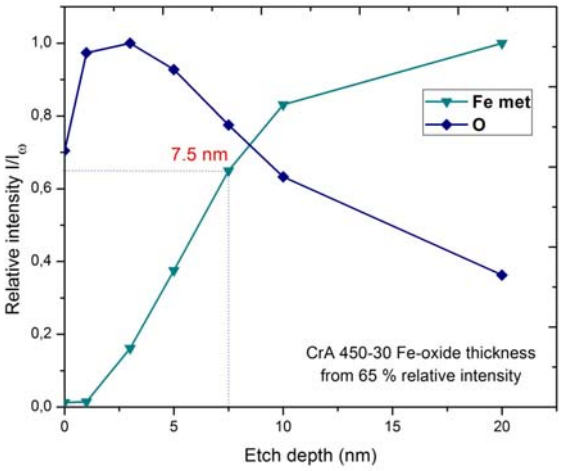

Fig.3. Normalized Fe metal and oxide intensities vs. etch depth plot indicating the Fe oxide thickness at 65% relative Fe intensity for the delubricated sample.

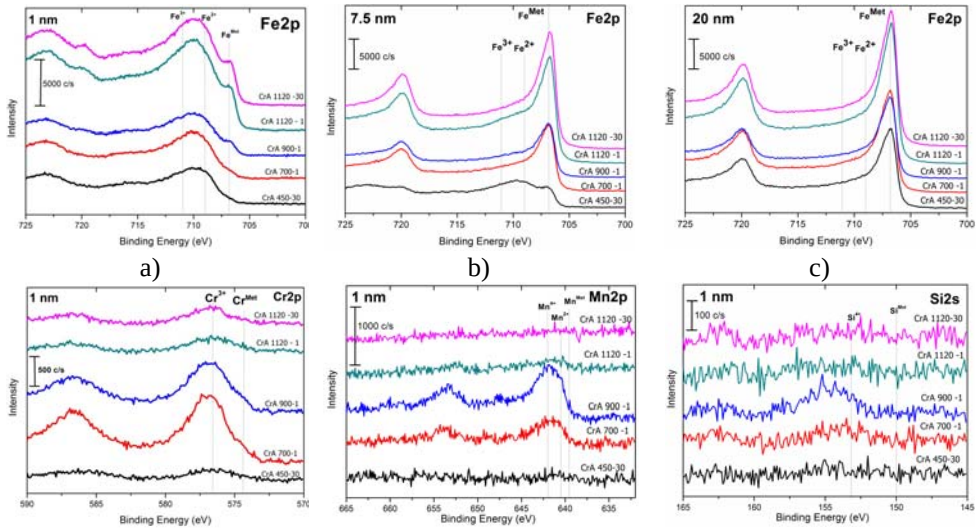

Fig.4. XPS narrow scans of Fe2p peak at etch depths of 1 nm (a), 7.5 nm (b) and 20 nm (c) and spectra for Cr2p peak at 1 nm (d), Mn2p at 1 nm (e) and Si2s at 1 nm (f). Results refer to the analysis on the fractured samples heated following the different procedures in Table 1.

As emphasized above, there is no meaning of evaluation of the iron oxide thickness for the samples heated to sintering temperature or the sintered one, since the exposure of the fracture surface to the air would mostly contribute to the iron oxide layer formation. The measured oxide thickness of 7.5 nm for the sample after delubrication is almost the same as typical value for the base powder (6-7 nm). In order to assess the chemical state of the elements, high energy resolution spectra were obtained for the

elements of interest. Spectra for Fe and Cr are shown in Fig.4. It can be observed that the Fe and Cr peaks have contributions predominantly from their respective oxides on the surface (a) and (d). Chromium does not indicate surface enrichment after delubrication and is present in the form of Cr-rich oxide particles, typical for the base powder [1-2].

The high resolution scans obtained for the samples after slight etching (1 nm) are shown in Fig. 4 together with the spectra for Fe after ion etching to 7.5 and 20 nm. The first row figures indicate that there is mainly contribution from the metallic state of Fe after 7.5 nm etching except for the just delubricated sample. After 20 nm of ion etching, only metal peaks for Fe are observed. Concerning Cr, there is significant increase in chromium cation contribution from oxide state at 700 °C that decreases with temperature and sintering time. The reason is the mass transfer of Cr to the powder surface with following oxidation. It is also important to emphasize the enrichment of Mn on the powder surface that indicates highest intensity at 900 °C. Contribution of Mn to the oxide composition decreases with the temperature and sintering time, similar to Cr. However, Mn enrichment is observed at higher temperature than the one for Cr. Silicon is present only in trace amount and hence difficult to quantify, especially at higher temperatures and etch depth. Si and Mn are only found in their oxide state for all etch depths.

This trend is described by the relative cation concentration profiles, see Fig.5a-e for the samples studied. Results show that at 450 °C powder is covered predominantly by Fe oxide layer with the presence of Cr-oxide and traces of Mn-Si-oxide, almost identical to the surface oxide composition of the base powder before heating. After heating to 700 °C, higher fractions of cations of Cr, Mn and Si are detected. This fact is connected to the incomplete reduction of iron oxide between the inter-particle necks as shown in model [13] that results in its transformation into more stable Cr-Mn-Si oxides during heating stage. This effect is even more evident for the sample heated to 900 °C.

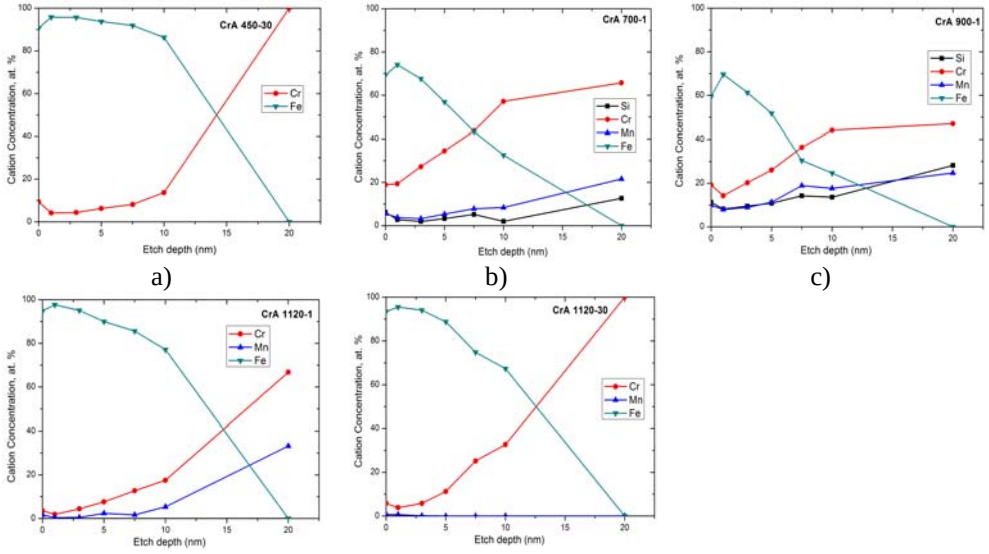

Fig.5. Relative cation concentrations at different etch depths of fractured surfaces of heated (a-d) and sintered (e) samples.

The temperature range between 700 and 900 °C constitute important range for the oxide transformation [14]. Early reduction of the Fe oxide results in the growth of point and line contacts between powder particles, as observed for sample just heated to 700 °C, and following formation of the necks at 900 °C, see Figs. 6a-b. The graphite is still present in the latter case showing that the carbon dissolution occurs only above 900°C when the Fe oxide is supposedly fully removed and base powder matrix is also transformed into austenite.

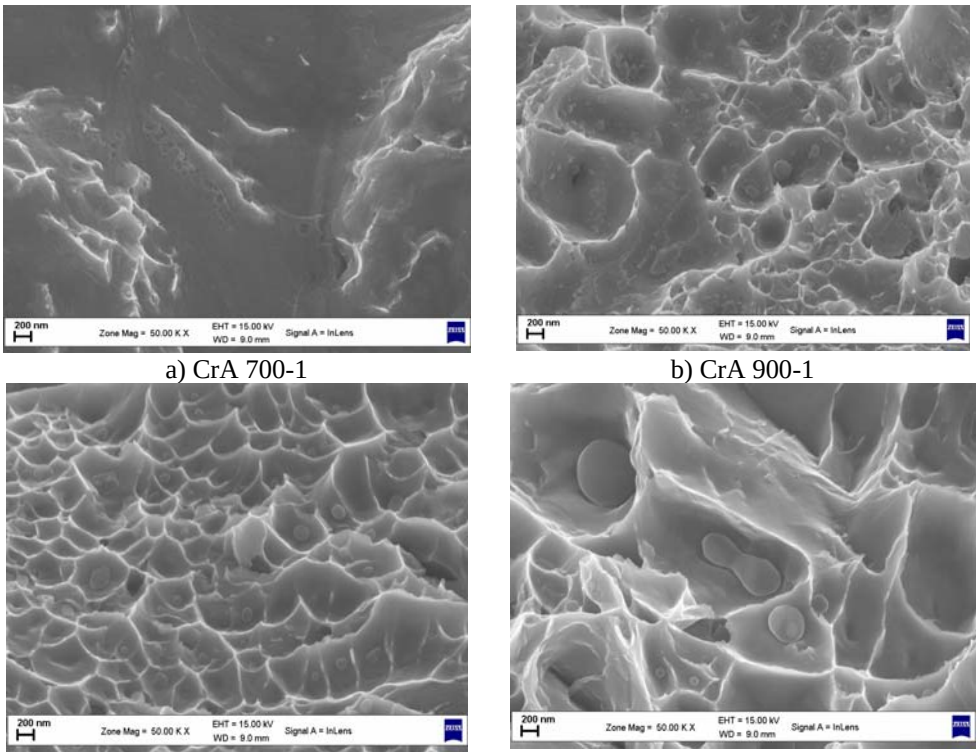

a) CrA 700-1 b) CrA 900-1

c) CrA 1120-1 d) CrA 1120-30

Fig.6. Fracture surfaces of the CrA+0.5 C compacts, showing the development of inter-particle necks at different stages of heating while sintering in 90% N_2/10 %H_2 atmosphere.

Some residual oxides were observed on the fracture surface of samples heated to 900 °C. As can be seen from Fig. 6b, these are found to be localized mostly at developing inter-particle necks as evidenced by the micro-dimple character of the fracture surface. Such oxide particles are supposed to be enclosed during the early growth of the inter-particle necks, as described in [13]. It can be assumed that extent of such enclosure significantly influences the strength of the necks. Formation and development of the oxide particles and their chemistry is described in details elsewhere [13]. At higher temperature and after sintering, there is a significant reduction of the thermodynamically stable oxide particles. Also, after sintering there are well developed inter-particle necks that are evident from the fracture surface appearance, indicating inter- and trans-particle ductile fracture characterised by deep dimples as seen in Fig. 6c-d. Coalescence of smaller oxide particles into agglomerates at sinter necks are seen after sintering, see e.g. Fig. 6d. This phenomenon is a result of the transformation of spinel oxide as discussed elsewhere [7,14].

The EDX analyses of the oxide inclusions revealed in the inter-particle necks on the fracture surfaces show that these are enriched in Cr and Si as well as Mn, see Fig. 7a-c. With increasing temperature, see Figs. 7a-c, the amount of Cr in the oxide particulates tend to be less, while level of Si and also Mn appears to be higher. Hence, this indicates change in oxide inclusions chemistry as expected from the thermodynamic stability point of view.

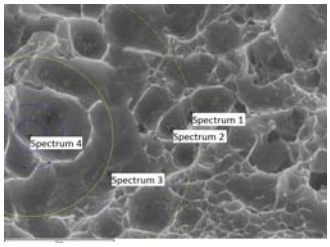

a) CrA 900-1

	O	Si	Cr	Mn	Fe	Total
Sp1	24.8	3.4	5.9	3.0	62.9	100
Sp2	9.4	2.5	2.0		86.1	100
Sp3	9.5	1.8	2.2		86.5	100
Sp4	3.5		2.1		94.4	100

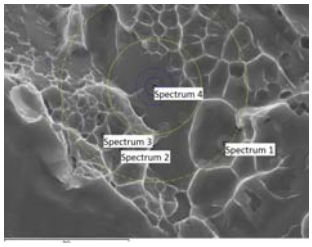

b) CrA 1120-1

	O	Si	Cr	Mn	Fe	Total
Sp1	38.7	5.1	1.2	7.2	47.8	100
Sp2	17.1	5.0	2.0	4.2	71.7	100
Sp3	19.2	6.3	1.8		72.7	100
Sp4	1.6		2.0		96.4	100

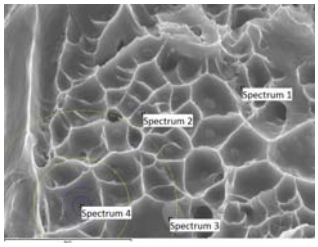

c) CrA 1120-30

	O	Si	Cr	Mn	Fe	Total
Sp1	32.4	5.8	4.3	2.1	55.4	100
Sp2	18.8	5.7	1.8		73.7	100
Sp3	42.7	7.8	0.5	9.4	39.6	100
Sp4	1.9		2.1		96.1	100

Fig.7. EDX analyses of the observed residual oxides/oxide inclusions inside the inter-particle necks in samples heated to 900°C (a), 1120°C (b) and after sintering (c).

CONCLUSIONS

Sintering in hydrogen-containing atmosphere leads to effective reduction of the iron oxide layer that initiates the early development of inter-particle necks. The temperature range between 700 and 900 °C is the crucial stage where the carbothermal reduction has low intensity but mass transfer of alloying elements is enforced, which brings risk of formation of stable oxides and their enclosure inside the forming necks. The enrichment of Mn and Si is observed inside inter-particle necks after heating to 900 °C, even if they are present in a trace amount in the alloy. These elements actively participate in oxide transformation, substituting Fe and even Cr at high temperatures. This oxide transformation from one kind to another occurs with increasing temperature and is driven by the difference in the stability of different oxides at respective temperatures during sintering process. Successful sintering of lean Cr-alloyed powder relies on the use of proper atmosphere control and adjusted temperature profile during the sintering cycle. Thus enabling PM parts manufacturers to achieve tailored properties suitable for high performance applications.

Acknowledgements

The authors would like to thank LIGHTer initiative by VINNOVA (Swedish Agency for Innovation Systems) and Sustainable Production Initiative of Chalmers Area of Advance in Production for financial support. Höganäs AB is acknowledged for scientific cooperation and permission to publish this research.

REFERENCES

[1] Karlsson, H.: PhD Thesis. Chalmers University of Technology, 2005
[2] Chasoglou, D.: PhD Thesis. Chalmers University of Technology, 2012
[3] Chasoglou, D., Hryha, E., Nyborg, L. In: Proc. EURO PM 2011, p. 111
[4] Chasoglou, D. et.al.: Appl. Surf. Sci., vol. 268, 2013, p. 496
[5] Hryha, E. et.al.: Appl. Surf. Sci., vol. 256, 2010, p. 3946

[6] Danninger, H. et.al.: Powder Metall. Prog., vol. 2, 2002, p. 125
[7] Kremel, S., Danninger, H., Yu, Y.: Powder Metall. Prog., vol. 2, 2002, p. 211
[8] Bergman, O.: Powder Metall., vol. 50, 2007, p. 243
[9] Danninger, H., Gierl, C.: Science of Sintering, vol. 40, 2008, p. 33
[10] Hryha, E., Nyborg, L.: Powder Metall. Prog., vol. 11, 2011, p. 42
[11] Chasoglou, D., Hryha, E., Nyborg, L. In: Proc. WORLD PM 2010. Vol. 2, p. 3
[12] Nyborg, L., Nylund, A., Olefjord, I.: Surf. Interface Anal., vol. 12, 1988, p. 110
[13] Hryha, E., Nyborg, L.: Metall. Mater. Trans. A, vol. 45, 2014, p. 1736
[14] Chasoglou, D., Hryha, E., Nyborg, L.: Powder Metall, vol. 11, 2011, p. 32